Effects of grazing ballistic impacts on combat helmets and behind helmet blunt trauma

BONEVA, Gabriela, NORTON-HEWINS, Kate, HAZAEL, Rachael, BROCK, Fiona and THAWANI, Bonny

Published version

BONEVA, Gabriela, NORTON-HEWINS, Kate, HAZAEL, Rachael, BROCK, Fiona and THAWANI, Bonny (2023). Effects of grazing ballistic impacts on combat helmets and behind helmet blunt trauma. In: COGHE, Frederik, (ed.) 33rd International Symposium on Ballistics. DEStech Publications, Inc, 1071-1082.

The Effects of Grazing Ballistic Impacts on Combat Helmets and Behind Helmet Blunt Trauma

Authors: Gabriela Boneva
Kate Norton-Hewins[1]*,
Rachael Hazael,
Fiona Brock
Bonny Thawani

PAPER DEADLINE: 01-07-23

PAPER LENGTH: ****MAXIMUM 12 PAGES****

[1] Cranfield Forensic Institute, Cranfield University, Defence Academy of the UK, Shrivenham, Swindon, SN6 8LA, United Kingdom
* Corresponding author. E-mail address: K.Norton-Hewins@cranfield.ac.uk

The current work experimentally studies the damage and injuries caused by grazing gunshot impacts on contemporary composite combat helmets. This study deduces that four failure modes are likely to occur on the protection system after impact of such nature. Micro-CT scans of the synthetic skulls used in these experiments do not show cranial fractures and surface damage, suggesting that the researched combat helmets efficiently dissipate the impact energy from multiple shots at multiple locations. The present research also proves that projectiles impacting a combat helmet at an oblique angle are likely to follow its geometry, rather than travel in a straight motion.

INTRODUCTION

The main causes of military traumatic brain injury are head injuries caused by violent impact, bullet penetration, or shock waves. Although the rapid advancements and innovations in weaponry, methods of combat, and greater utilization of unmanned warfare reduce the number of wounded soldiers, they do not decrease the risk of traumatic brain injury in soldiers [1]. The head represents approximately 9% of the body area, but is representative of

around 20% of the injurious impacts in combat environments [2]. Modern helmets and body armour have the basic function of stopping penetration from projectiles and fragments. The second main function of ballistic protection wear is the effective dissipation of the kinetic energy from the projectile, ensuring only minor amount of it is transferred onto the body [3]. Backface deformations (BFD) occur when the penetration of a projectile is stopped by the ballistic protection but the high energy from the projectile causes deformations on the protective system which may lead to non-penetrating trauma [4]. When a helmet is struck by a projectile and penetration does not occur, a conical bulge is formed at the backface which is required to not exceed a critical value [5]. If the BFD exceeds the critical values, behind armour blunt trauma (BABT), or more specifically behind helmet blunt trauma (BHBT), may occur.

Composite helmets provide increased blunt impact protection; however, the increased ballistic mass efficiency of the materials led to a greater susceptibility of the body armour of BFD upon impact [6]. Modern helmet shells have thicknesses of between 5mm and 10mm [7],and pad suspension systems are present to increase the comfort of the wearer and also provide protection from blunt forces with lower intensity than the impact forces from a non-penetrative ballistic event. The understanding of energy transfer, momentum from strike face to backface of the helmet, and the interaction between the BFD and the head are crucial for the decrease of injuries and increase of survivability at the battlefield [6].

This work experimentally studies the effects of BHBT upon tangential ballistic impact onto composite combat helmets and performs post-impact cranial analyses to investigate the occurred fractures, if any, caused by the BFD. The current study also examines the projectile behaviour after grazing impact with the protection system, allowing a better understanding of the potential injuries both for the target and nearby personnel.

Ballistic protective systems defeat the projectile by absorbing its kinetic energy and converting it to some sort of deformation of the material, preventing the full penetration of the armour system [8]. The objective of ballistic fabrics is to bring the

velocity of the projectile to zero before complete penetration occurs. The kinetic energy from the stress waves formed upon impact is dissipated through backface deformations, friction between the fibre and the projectile, shear plugging, and fibre deformations and breakages [5]. If the dynamic tensile strain of fibre is exceeded upon impact, the fibre breaks and the next layer absorbs part of the non-dissipated energy. Complete penetration occurs when all layers fail. Although modern helmets provide enhanced ballistic protection against penetrating injuries, the increased strength and toughness and lighter weight of the used materials tend to increase the BFD [6].

Two finite element studies [9,10] investigate the ballistic performance of the Advanced Combat Helmet (ACH) upon impacts with 9mm full metal jacket rounds at different locations of the protective system. The results from Palta et al. [9] suggest that the BFD values vary at the different impact locations due to the curvature of the helmet, and report that lower BFD values occur at lateral impacts of 45° as compared to the ones at 90° impacts. Palta et al. [9] report delamination, compressive matrix damage, fibre breakage, and matrix cracking, as the first three failure modes are also reported by Li et al. [10]. Although useful to understand the expected failure modes of the ACH, a limitation of both numerical studies is that they are validated against data obtained from literature rather than experimentally. Furthermore, the numerical model by Li et al. [10] is validated against a different type of helmet (PASGT) rather than the ACH, and the two helmets have different geometry which impacts the ballistic performance of the systems.

Backface dynamic deformations in response to a ballistic impact can lead to BHBT, the severity of which varies from superficial abrasions and bruising to fractures and brain injuries [11]. The stand-off between the protection system and the head of the wearer is highly limited, allowing only minuscule BFD without the armour impacting the wearer. Rafaels et al. [4] study the head injuries observed from BFD on UHMWPE (Ultra High Molecular Weight Polyethylene) helmets by using postmortem human subject specimens. The specimens are impacted with 9mm FMJ rounds with velocities between 405 m/s and 459 m/s at the parietal region (sides and top of the cranium). Linear and depressed fractures are present on the specimens, with the linear fractures resulting from the global energy transfer from the impact and the depressed fractures resulting from the local contact with the projectile. Linear fractures are typically associated with direct penetrating trauma; however, their joint presence with depressed fractures can be used to distinguish BHBT injuries from direct penetration ones [4].

Ricocheted bullets upon low-angle impact lose part of their velocity but may still be able to cause gunshot injuries; however, a smaller depth of penetration may be expected [12,13]. The capacity of ricocheted bullet to cause injuries depends on its mass, shape, and post-impact velocity, as the estimated post-impact velocity of a ricocheted projectile to perforate human skin and tissue is minimum 61 m/s [13].

MATERIALS AND METHODS

Eight Synbone® synthetic solid foam skulls with mandibles and visor attachments were partially filled with 10% ballistic gelatine. Eight example composite

combat helmets[2], sizes small and medium, were fitted onto the skull samples. The samples were secured onto a mounting table.

According to NATO AEP 2920 [14], when the performance of a helmet is evaluated, a backface signature (BFS) material (i.e. a clay head rig) is used to establish whether the ballistic threat was defeated. Complete helmet penetration is recorded when the projectile or fragments from it are present in the backface signature material, or a hole passes through the shell. The presence of non-metallic materials from the helmet on the backface signature material do not indicate complete penetration.

Post-firing, the external damage of the helmet shells and the padding suspension systems was visually examined and photographed. The padding was removed and the BFD were assessed. Although no BFS material was used in this study, the performance of the helmet was evaluated using NATO AEP 2920 [14] criteria, and the presence of projectile fragments in the targets and holes through the shells was assessed using micro-CT scanning and flashlights respectfully.

Two types of projectiles with a total of 28 rounds were used in this study. For the first 24 shots, 7.62 x 39 mm full-metal jacket (FMJ) stainless steel core ammunition was used. For the final 4 shots, 7.62 x 51 mm NATO FMJ lead core ammunition was used. These rounds were selected as they represent the most predominant military rifle rounds in service globally, thus enabling the realistic representation of the helmet deformations and personnel injuries likely to be seen in a combat environment [15]. The testing was performed in an indoor testing fire range using fixed barrels from a proof mount. The targets were positioned 10m from the fixed barrel. Doppler radar was positioned on the right-hand side of the barrel.

The aim of the research is to accomplish grazing gunshots on the shells without full penetration of the helmet system, thus, the angles of impact were tangential. Figure 1 (A) shows the impact locations. Four of the samples were shot three times (one lateral front shot A1, one central front shot A2, and one lateral rear shot A3), and four of the samples were shot four times (one lateral front shot b1, one off-centre top front shot B2, one off-centre top rear shot B3, and one lateral rear shot B4). Seven samples were shot with 7.62 x 39 mm rounds, and one sample was shot with 7.62 x 51 mm. The mean velocity of the 7.62 x 39 mm shots was 708.4 m/s (between 656.5 m/s and 734.3 m/s), and the mean velocity of the 7.62 x 51 mm was 803.3 m/s (between 797.1 m/s and 806.5 m/s). Phantom V12 high-speed camera was placed approximately 1.5 m from the samples and was used to obtain footage of the firings.

[2] The make of the helmets is not mentioned for security reasons.

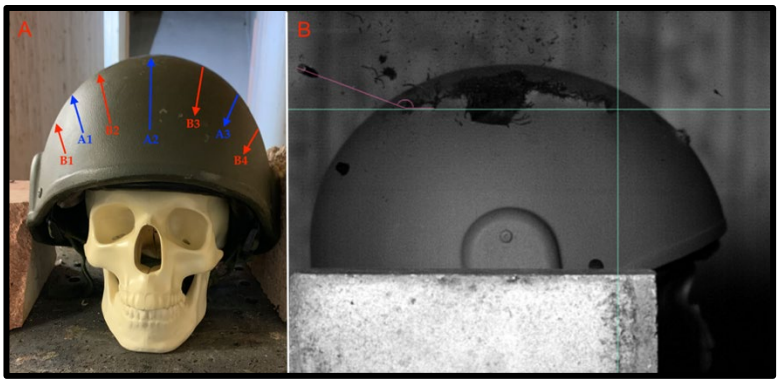

Figure 1 A: Group A showing the impact locations of the samples shot three times. Group B showing the impact locations of the samples shot four times. Figure 1 B: PCC Instant Measurement 2 points setting and active axes to determine entrance and exit angle difference.

The angular difference between the entrance point and the exit point of the projectile is approximated by drawing a straight line from the entrance point and following the direct curvature of the helmet. Another line, again from the entrance point, is drawn to the exit point (Figure 1B). The formed angle is measured using a protractor. Due to the geometry of the helmet, the obtained measurements are only an approximation of the difference between the entrance and exit points of the projectile.

The current study did not record the post-impact velocities of the projectiles, but the study by Braga et al. [16] can be used to estimate the residual post-impact velocity of the projectiles. Braga et al. [16] report initial velocities between 843 m/s and 861 m/s, and the residual velocities post-impact with the thinnest studied fabric (8mm) is reported to be 835 m/s. The measured residual velocity post-impact with 25mm laminate is 732 m/s, for 38mm thickness is 194 m/s, and for 50mm is 0m/s [16].

The helmets were impacted at 90° angles, and the high-speed footage from the experimental testing was used for measuring the ricochet of the projectile after exiting the helmet. Phantom Camera Control (PCC) software (v. 3.6) is used to analyse the data. A calibration video with a forensic scale was taken, and the footage was calibrated at 0.624 mm/pix. After calibration, axes lines with a set origin the tip of the projectile at the last frame before impact were put.

The X-axis at the point of exit was used to measure the exit angle of the projectile by using the 2 points instant measurement setting of the software. The last frame where the projectile is visible after leaving the helmet is used for measuring the exit angle. The 2point instant measuring is set at the exit point of the helmet on the X-axis and extended to the projectile (Figure 1B). The ricochet angles are calculating by subtracting the measured angle from 180°.

Observations of the sub-surface changes of the Synbone® microstructures upon the ballistic impacts were made by using a Nikon Metrology X-TEK H225 micro-computed tomography (micro-CT) scanner with a tungsten reflectance target operating in panel scan mode. The working conditions were: 100 ms exposure time, 110 kV, 70 µA. The instrument was set to collect data at 720 projections, with two frames taken at each projection, and a resultant voxel size of 125.0 µm. Inspect-X software (v. 3.1.12) was used for data collection, CT Pro 3D software (v. 3.1.12) was used for data reconstruction, and VG StudioMax software (v. 2.1) was used for image visualisation and manipulation. TIFF image stacks were created in 0.13 mm slice in three directions:

top to bottom, right to left, and front to back. The three following samples were selected for CT-scanning: two impacted with 7.62 x 39 mm rounds (one shot three times and one shot four times), and the one sample impacted four times with 7.62 x 51 mm. The software package ImageJ (v. 1.8.0) was used for the visualisation of the TIFF stacks.

RESULTS

The methods of entrance and exit point difference approximation and ricochet angles measuring are described above. The approximated angular deviation varies between 0° and 50°, with 20° accounting for the greatest portion of approximated deviation (*28.6%*). The calculated ricochet angles vary between 2.49° and 35.33°. Impacts with ricochet angle below 10° account for *17.9%* (*n=5*) of the total shots; between 10° and 15° for *21.4%* (*n=6*); between 15° and 20° for *3.6%* (*n=1*); between 20° and 25° for *21.4%* (*n=6*); between 25° and 30° for *14.3%* (*n=4*); between 30° and 35° for *17.9%* (*n=5*); and impacts with ricochet angles above 35° account for *3.6%* (*n=1*).

The recorded velocities of the 7.62 x 39 mm projectiles are between 686.5 m/s and 734.3 m/s, with average velocity of 708.4 m/s. The recorded pre-impact velocities of the 7.62 x 51 mm are between 797.1 m/s and 806.5 m/s, with average velocity of 803.3 m/s.

As seen on Figure 1 A, the impact locations are: front lateral (*28.6%, n=8*), central front (*14.3%, n=4*), rear lateral (*28.6%, n=8*), front top off-centre (*14.3%, n=4*), and rear top off-centre (*14.3%, n=4*). The observed shell damage can be categorised into the following groups: partial penetration (*50%, n=14*), superficial graze (*17.9%, n=5*), graze through the shell (*3.6%, n=1*), complete penetration (*21.4%, n=6*), and partial shell cracking (*7.2%, n=2*).

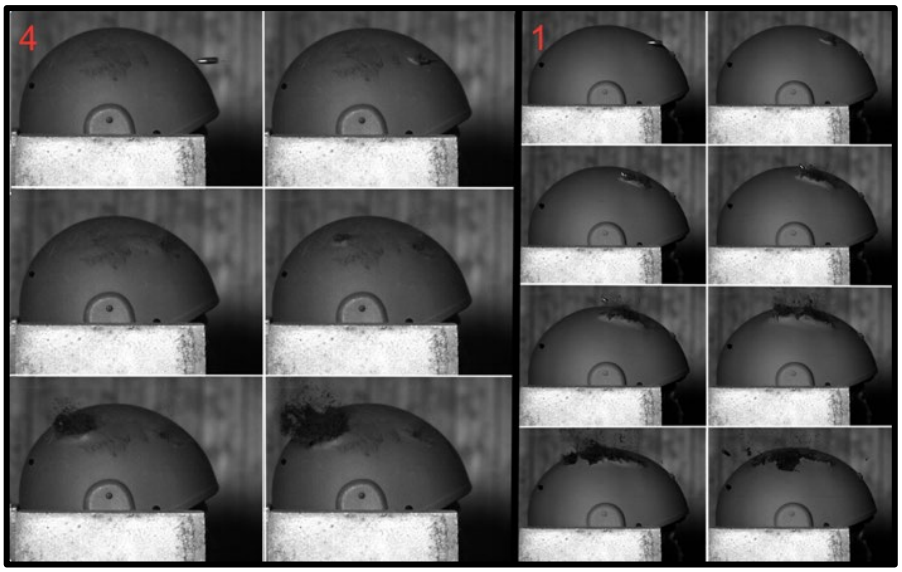

Figure 2 Frames from the high-speed footage. Left side: shot 4 where the projectile partially penetrates the shell at the front and exits at the read rise of the helmet without fully penetrating the padding. Right side: shot 1 where the projectile grazes on the shell laterally.

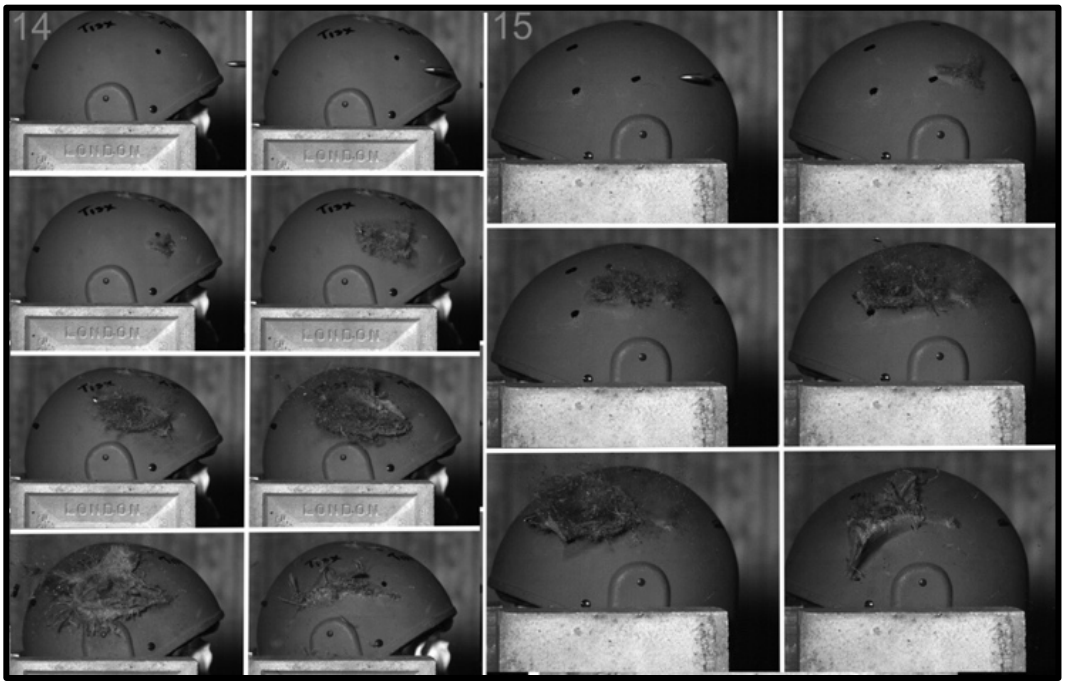

Figure 3 Frames from the high-speed footage. Left side: shot 14 where the projectile partially perforates the shell and follows its curvature. Right side: shot 15 where the projectile penetrates through the shell and follows its curvature, leaving a complete shell penetration.

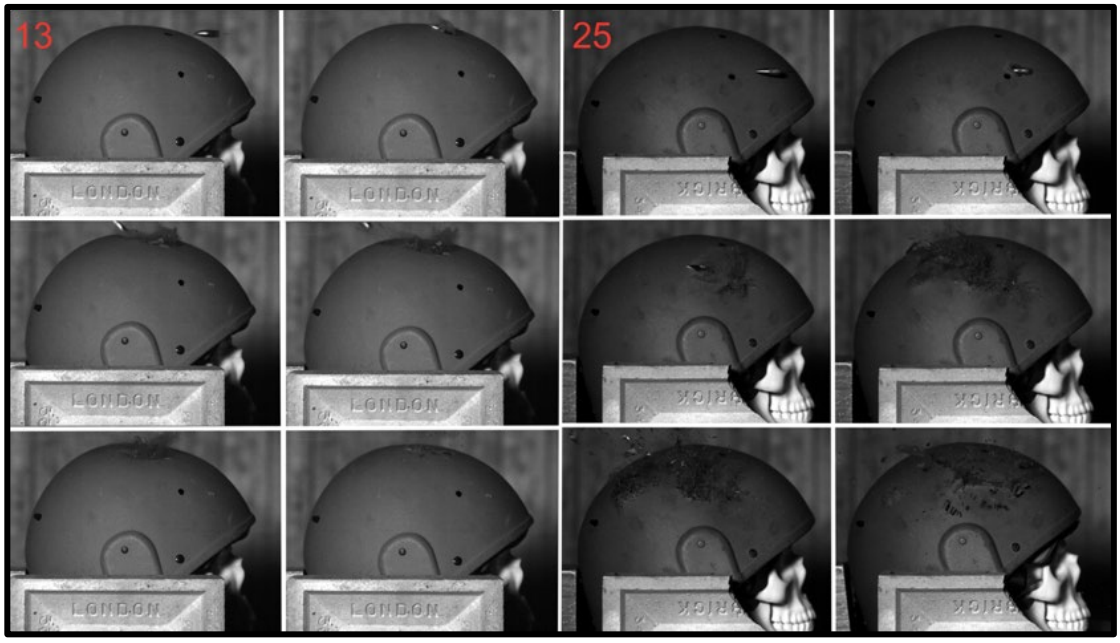

Figure 4 Frames from high-speed footage. Left side: shot 13 where the elastic bending of the shell upon the impact can be seen. Right side: shot 25: 7.62 x 51mm NATO ammunition.

Four types of outer-face padding damage are observed upon impacts: grazing damage (*28.6%*, *n=8*), surface perforation (*7.1%, n=2*), compressive damage (*25%, n=7*), compressive grazing damage (*14.3%, n=4*), and *25%* (*n=7*) of the samples did not show any outer-face padding damage. Three-quarters (*n=21*) of the samples did not show any inner-face padding damage, and the remaining showed grazing damage (*14.3%, n=4*), compressive damage (*7.1%, n=2*), and partial tearing (*3.6%, n=1*).

Upon post-firing examinations, four failure modes are observed on the shells: delamination, fibre breakage, matrix cracking, and compressive matrix damage. The damage caused by all shots, except of Shots 2 and 26, shows characteristics of delamination. More than half of the samples expose compressive matrix damage characteristics. On Shots 2 and 26, only compressive matrix damage is observed due to the surface level impacts. The level of damage observed on the padding suspension systems varies, with only 25% of the samples exposing any degree of damage on the inner face of the padding. However, 75% of the samples show some degree of outer face padding damage.

Upon visual examination, none of the skulls exhibited damage post-firing. Three skulls were examined using a micro-CT scanner. The examined samples were Sample 5 (Shots 13, 14, 15, 16), Sample 6 (Shots 17, 18, 19, and 20), and Sample 8 (Shots 25, 26, 27, and 28). The three CT-scanned samples show similar traits of damage at the parietal area of cranium, which characterizes in spherical microstructural deformations.

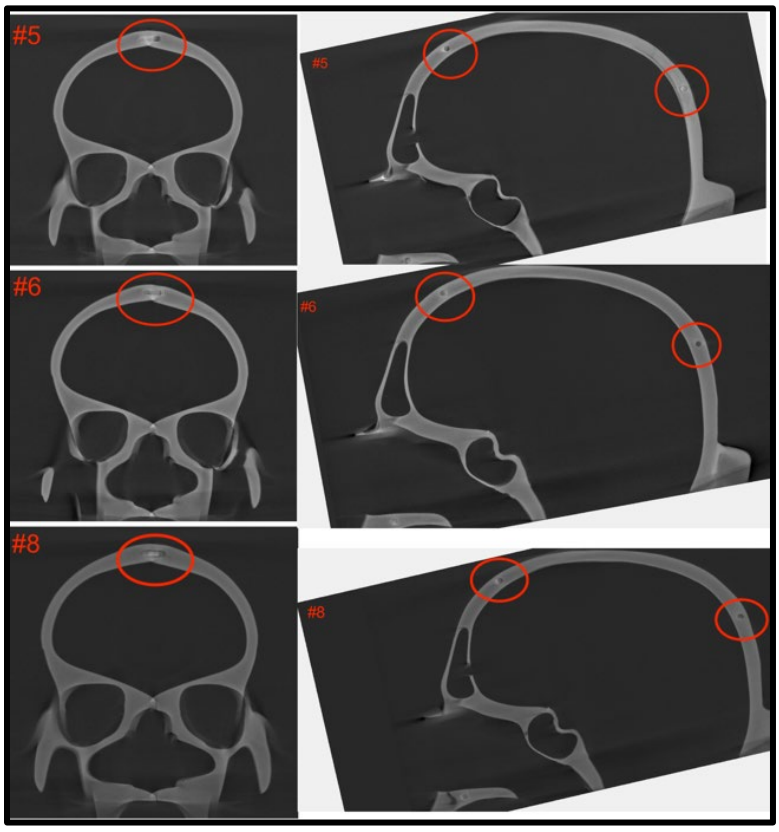

Figure 5 Micro-CT scan of skulls #5, #6, and #8, areas of damage is circled. Left column showing the front scans of the skulls (top to bottom: #5, #6, #8), right column showing the right scans (top to bottom: #5, #6, #8)

DISCUSSION

The angular deviation between the entrance and exit points suggests that for tangentially impacting gunshots, the projectiles follow the curvature of the helmets to an extent, rather than travel in a straight motion through the system. A confirmation of this can be achieved by visually assessing the gunshot damage on the helmets and by approximating the difference between the entrance and exit angles. Although grazing gunshots at oblique angles relative to the geometry of the helmet were fired, the entrance angle of the projectile was 0° due to the small cross-sectional area of the nose of the projectile and the perpendicular firing.

No angular difference is observed for Shots 8 and 10 which impacted the central front area of the helmets. Due to the oblique angles of impact and the curvature of the shell, the projectiles follow the geometry of the shell rather than causing a complete penetration of the system. The entrance-exit angular difference is in the range between 0° and 50°. The 20° deviation accounts for the greatest portion of the approximated angles (*28.6%*), followed by 30° (*17.8%*), and 25° (*10.7%*). Deviations of 0°, 35°, and 45° are equally represented (*7.1%* each). The following deviations are also equally represented, *3.6%* each: 7°, 10°, 15°, 18°, 40°, and 50°.

No specific angular deviation distribution is observed at the different impact location. This implies that the difference between the entrance and exit angles is more dependent on the helmet geometry at the exact area of impact rather than on the impact angle alone (which, as mentioned, is 0°). Future research should focus on the in-depth study of the angular deviation between the entrance and exit point of the projectile by assessing the impact angle in relation to the curvature of the helmet at the exact impact point.

The calculated ricochet angle values vary from 2.49° to 35.33°. The majority of the projectiles deflect upwards after leaving the helmet, and only a small portion of the projectiles deflect downwards. The variability of the measured ricochet angles indicates that the angles of impact relating to the helmet geometry have a paramount role in the behaviour of the projectile after leaving the headwear. The obtained high-speed footage presents that the helmet shells may behave elastically upon non-penetrating oblique impacts (e.g. Shot 13, Figure 4) and deflect the projectile upwards after impact.

A limitation of this study is the lack of recorded post-impact velocities of the projectiles. Thus, the potential injuries to nearby personnel caused by the ricocheted projectiles in this study cannot be fully discussed. As stated by Yong [13], the minimal post-impact velocity required for skin and tissue penetration is 61 m/s. As abovementioned, the shell thickness of modern combat helmets is between 5mm and 10mm [7], and the study by Braga et al. [16] can be utilized for the estimation of the residual velocity of the projectiles in this study. As stated by Braga et al., for a 7.62 x 51 mm projectile impacting an 8mm thick aramid laminate, the velocity loss post-impact is 3%. Taking the mean initial velocity recorded in the current study (708.4 m/s [3]), the estimated residual velocity post-impact is 687.1 m/s. This estimation does not consider the specific geometry of the helmets, and the reference values taken from the study of Braga et al. are obtained using different ballistic materials and projectiles.

Although it can be hypothesized that ricocheted bullets and fragments after tangentially impacting a composite combat helmet may cause injuries to personnel close

[3] Mean applies for the 7.62 x 39 mm shots only.

to the target, discussions of the levels of potential injuries are beyond the scope of this study. Further research including the recording of projectile velocity and using witness boards should be conducted for a greater understanding of the possible injuries induced by ricocheted projectiles upon tangential impact with combat helmets.

Only three of the 7.62 x 39 mm shots resulted in complete shell penetration paired with padding damage. As mentioned earlier, ballistic impacts at 45° result in smaller BFD values than the ones at 90° [10]. The shots in the current study are tangential, thus of a low impact angle. The reported by Li et al. [10] lower BFD values may be indicative for overall lower damage levels on the helmet system. Thus, it may be suggested that the low percentage of complete shell penetration recorded in the current study is due to the grazing nature of the impacts. None of the three shots that resulted in complete shell penetration impacted the central top area of the helmet: one of the shots was lateral (Shot 15), and two were front top off-centre (Shots 17 and 22). The numerical study by Li et al. suggests that greater BFD values are likely to be observed at the front central impacts. The reason for the discrepancy between the current study and the numerical study by Li et al. [10] may be the different geometries of the studied helmets and the different projectiles. Additionally, the precision of the current study is more limited than the one of the numerical study, which is due the application of fixed barrels on a proof mount and laser pointer aims. The laser pointer aim tends to deform because of the helmet curvature, which may negatively affect the accuracy of some of the shots. Thus, the likely reason for the recorded complete shell penetration shots is due to the decreased aiming accuracy, resulting in more direct shots at higher impact angles.

Four failure modes are observed on the helmet shells of the current study: delamination, fibre breakage, matrix cracking, and compressive matrix damage – the same failure modes reported in the numerical studies by Li et al. [10] and Palta et al. [9]. These failure modes are methods of energy dissipation and absorption which reduce the risk of injuries to the wearer.

The projectile behaviour upon impact can be briefly categorized into three groups: the projectile partially penetrates the shell and follows its curvature, leaving a visible damage track on the surface of the helmet (shots 1, 10, 14, 15, 19, 22); the projectile partially penetrates the shell and leaves none or minimal visible surface tracks on the shell with pronounced entrance and exit points (shots 3, 4, 5, 6, 7, 8, 9, 16, 17, 18, 20, 21, 23, 24); and the projectile impacts the shell at its very surface and leaves a minor grazing mark on the shell without detectable deformations (shots 2, 11, 12, 13). There is no observed correlation between the impact location and the post-impact damage or the projectile behaviour. The resultant padding damage varies, but complete padding perforation is not detected.

Minor plastic BFD was observed on 24 of the helmet shells upon removal of the padding suspension system. However, discussion of the backface signatures is beyond the scope of this study as synthetic skulls were used rather than backface signature material.

Three out of the four 7.62 x 51 mm shots (shots 25, 27, and 28) resulted in complete penetration of the shell. The high-speed footage shows greater levels of deformation of the projectiles upon impact as compared the ones observed on the 7.62 x 39 mm projectiles. The likely reason for this occurrence is the much softer material properties of the lead core 7.62 x 51 mm rounds as compared to the steel core 7.62 x 39 mm rounds. Although significantly fewer 7.62 x 51 mm shots were fired in this study

as compared to 7.62 x 39 mm ones, 75% of the larger rounds caused complete penetration of the shell and damaged the padding. The greater percentage of the complete penetration caused by the 7.62 x 51 mm rounds (*75%*) as compared to the complete penetration caused by the 7.62 x 39 mm rounds (*12.5%*) is likely due to the different in propellant energies and the mass of the propellants used in the two types of ammunition. A limitation of the current study is that only a limited amount of 7.62 x 51 mm ammunition was used and future in-depth research on the effects of propellant in different ammunition in the context of grazing gunshot impact on protective systems should be conducted.

The visual examination of the skulls suggests that no damage was caused by the ballistic impacts. In accordance with the findings of Daghfous et al. [17], these observations imply that there is no ballistic damage on the skulls, suggesting that the helmets efficiently dissipated the energy from multiple shots at multiple impact locations. However, the results from the micro-CT scanning show that all three of the scanned skulls have similar damage in the parietal and frontal areas (Figure 5). The phenomenon may be the resultant of multiple microstructure pores collapsing into one due to the impact; however, this is highly unlikely due to the lack of surface damage on the skulls. The used in the current study synthetic Synbone® skulls are manufactured by injection moulding, and the likely reason for the consistent damage seen on all three scanned skulls is a manufacturing defect in the area where the nozzle of the injection is inserted during manufacturing. Furthermore, identical defects are observed at the maxilla bone where no ballistic impacts occurred. Additionally, Daghfous et al. [17] state observing bone fragments inside the cranium, which is not seen on any of the micro-CT scans from the current study. This further indicates that the observed damage is rather a manufacturing defect than ballistic impact damage.

A limitation of the current study is that the synthetic skulls were not scanned before the testing; thus, a comparison between the pre- and post-firing scans cannot be made. Additionally, the skulls used in this study were crania with mandibles which are anatomically correct models used mainly in the medical field for trainings, and their behaviour under ballistic impact may not be an accurate representation of the behaviour of human crania under the same conditions. For better understanding of the potential injuries that may occur upon tangential ballistic impact on combat helmets, experimental testing using postmortem human subjects should be conducted.

CONCLUSION

A total of 6 out of 28 impacts in this study resulted in complete shell penetration. 75% of the shots caused damage to the outer face of the padding and 25% caused minor damage to the inner face of the padding as well. Although the observed levels of inner face damage are minor, the application of additional helmet cushioning should be considered.

As of the results of the current study, tangential gunshots partially penetrate the shell and follow its curvature without causing full system penetration depending on the geometry at the exact area of impact. This suggests that greater levels of survivability and decreased amounts of injuries are likely to be observed if personnel sustain grazing gunshot impacts at their helmets as compared to direct impacts. Further research on the

impact angles in relation to the helmet geometry should be performed for more in-depth understanding of the angular deviation between entrance and exit points.

The assessment of ricochet angles from the high-speed footage shows variability between 2.49° and 35.33°, as the majority of the projectiles are deflected upwards post-impact. The wide range of ricochet angles suggests that personnel in close proximity to the target may sustain ricochet gunshot injuries depending on their distance from the target and their elevation relating to the target. Future work in this area may include experimental testing using witness boards placed around the target and obtaining the velocity of the ricocheted projectiles to gain a better theoretical understanding of the ricochet injuries that may be sustained by nearby personnel.

Various levels of delamination, fibre breakage, compressive matrix damage, and matrix cracking were observed. Minor plastic BFD were also recorded upon removal of the padding suspension systems. Three of the 7.62 x 39 mm and three of the 7.62 x 51 mm rounds caused complete shell penetration. The observed failure modes and the low number of complete shell penetrations suggests that the helmet systems successfully dissipated the energy from multiple 7.62 x 39 mm shots at multiple locations. Future work may involve testing with a wider variety of ammunition and focusing on the effects of different propellant types and quantities in relation to the sustained helmet damage. The application of head rigs may be used for assessing the backface signatures of tangential shots.

There is no damage observed on the skulls upon visual examination. The micro-CT scanning of the three skulls showed reoccurring damage with similar characteristics in the same areas of the crania. Due to the lack of surface damage and the consistency of the damage seen on the scans, the observed characteristics are likely to be manufacturing defects. Thus, no ballistic damage was recorded on the micro-CT scanned skulls, indicating that the helmets have efficiently dissipated and absorbed the energy from multiple impacts at multiple locations. Future research concerning the potential injuries of tangential ballistic impacts on a helmet may involve postmortem human subjects to test the findings of the current study. Furthermore, the potential traumatic brain injuries caused by tangential gunshots on victims wearing combat helmets may be studied.

Overall, the current study concludes that the example composite combat helmets used in these experiments are capable of efficiently dissipating multiple 7.62 x 39 mm FMJ stainless steel core gunshot impacts at different locations without full failure of the protection system and detectable cranial fractures.

DATA AVAILABILITY STATEMENT

Data and further details available on request from the authors.

REFERENCES

1. Kong, L. Z., Zhang, R. L., Hu, S. H., & Lai, J. B. (2022). Military traumatic brain injury: a challenge straddling neurology and psychiatry. In *Military Medical Research* (Vol. 9, Issue 1). BioMed Central Ltd. https://doi.org/10.1186/s40779-021-00363-y
2. Carey, M., Herz, M., Corner, B., McEntire, J., Malabarba, D., Paquette, S., & Sampson, J. (2000). Ballistic Helmets and Aspects of Their Design. *Neurosurgery*, *47*(3).

3. Prat, N., Rongieras, F., Sarron, J.-C., Miras, A., & Voiglio, E. (2012). Contemporary body armor: technical data, injuries, and limits. *European Journal of Trauma and Emergency Surgery*, *38*, 95–105.
4. Rafaels, K., Cutcliffe, H., Salzar, R., Davis, M., Boggess, B., Bush, B., Harris, R., Rountree, M. S., Sanderson, E., Campman, S., Koch, S., & Bass, C. (2015). Injuries of the Head from Backface Deformation of Ballistic Protective Helmets Under Ballistic Impact. *Journal of Forensic Sciences*, *60*.
5. Kulkarni, S. G., Gao, X.-L., Horner, S. E., Zheng, J. Q., & David, N. V. (2013). Ballistic helmets – Their design, materials, and performance against traumatic brain injury. *Composite Structures*, *101*, 313–331.
6. Freitas, C., Mathis, J., Scott, N., Bigger, R., & MacKiewicz, J. (2014). Dynamic Response Due to Behind Helmet Blunt Trauma Measured with a Human Head Surrogate. *International Journal of Medical Sciences*, *11*(5), 409–425.
7. Hamouda, A. M. S., Sohaimi, R. M., Zaidi, A. M. A., & Abdullah, S. (2012). 6.4. Design aspects of ballistic helmets. In E. Sparks (Ed.), *Advances in Military Textiles and Personal Equipment* (1st ed.). Woodhead Publishing Limited.
8. Abtew, M. A., Boussu, F., Bruniaux, P., Loghin, C., & Cristian, I. (2019). Ballistic impact mechanisms – A review on textiles and fibre-reinforced composites impact responses. *Composite Structures*, *223*.
9. Palta, E., Hongbing, F., & Weggel, D. (2018). Finite element analysis of the Advanced Combat Helmet under various ballistic impacts. *International Journal of Impact Engineering* , *112*, 125–143.
10. Li, Y. Q., Li, X. G., & Gao, X.-L. (2015). Modeling of Advanced Combat Helmet Under Ballistic Impact. *Journal of Applied Mechanics* , *82*.
11. Sarron, J.-C., Dannawi, M., Faure, A., Caillou, J.-P., Cunha, J. D., & Robert, R. (2004). Dynamic Effects of a 9 mm Missile on Cadaveric Skull Protected by Aramid, Polyethylene or Aluminum Plate: An Experimental Study. *The Journal of Trauma*, *57*, 236–242.
12. Haag, M., & Haag, L. (2011). Projectile Ricochet and Deflection. In *Shooting Incident Reconstruction* (Second). Elsevier.
13. Yong, Y.-E. (2017). A systematic review on ricochet gunshot injuries. *Legal Medicine*, *26*.
14. (NATO), N. A. T. O. (2016). *STANAG 2920 Classification of Body Armour: Procedures for the Evaluation and Classification of Personal Armour - Bullet and Fragmentation Threats Edition A Version 2*.
15. Jenzen-Jones, N. R., & Schroeder, M. (Eds.). (2018). Weapons Identification: Small-calibre ammunition. In *An Introductory Guide to the Identification of Small Arms, Light Weapons, and Associated Ammunition*. Small Arms Survey.
16. Braga, E. de O., Lima Jr., E. P., Lima, E. de S., & Monteiro, S. N. (2017). The Effect of Thickness on Aramid Fabric Laminates Subjected to 7.62 MM Ammunition Ballistic Impact. *Materials Research* , *20*.
17. Daghfous, A., Buzaidi, K., Abdelkefi, M., Rebai, S., Zoghlemi, A., Mbarek, M., & Rezgui Marhoul, L. (2015). Contribution of imaging in the initial management of ballistic trauma. *Diagnostic and Interventional Imaging*, *96*.